Discriminatory ability of next-generation tau PET tracers for Alzheimer's disease

Steven Y. Yap,[1,2,†] Barbara Frias,[3,4,†] Melissa C. Wren,[1,2,3,4] Michael Schöll,[5,6] Nick C. Fox,[6,7] Erik Årstad,[1,2] Tammaryn Lashley[3,4] and Kerstin Sander[1,2]

†**These authors contributed equally to this work.**

Abstract

A next generation of tau PET tracers for imaging of Alzheimer's disease and other dementias has recently been developed. Whilst the new compounds have now entered clinical studies, there is limited information available to assess their suitability for clinical applications. Head-to-head comparisons are urgently needed to understand differences in the radiotracer binding profiles.

We characterised the binding of the tau tracers PI2620, RO948, MK6240 and JNJ067 in human *post-mortem* brain tissue from a cohort of 25 dementia cases and age-matched controls, using quantitative phosphorimaging with tritium labelled radiotracers in conjunction with phospho-tau specific immunohistochemistry.

The four tau radiotracers depicted tau inclusions composed of paired helical filaments with high specificity, both in cases with Alzheimer's disease and in primary tauopathy cases with concomitant Alzheimer's disease pathology. In contrast, cortical binding to primary tauopathy cases without paired helical filament tau was found to be within the range of age-matched controls. Off-target binding to monoamine oxidase B has been overcome, as demonstrated by heterologous blocking studies in basal ganglia tissue. The high variability of cortical tracer binding within the Alzheimer's disease group followed the same pattern with each tracer, suggesting that all compounds are suited to differentiate Alzheimer's disease from other dementias.

Author affiliations:

1

1 Centre for Radiopharmaceutical Chemistry, Department of Imaging, University College London, London, UK

2 Department of Chemistry, University College London, London, UK

3 Queen Square Brain Bank for Neurological Disorders, Department of Clinical and Movement Neurosciences, Queen Square Institute of Neurology, University College London, London, UK

4 Department of Neurodegenerative Disease, Queen Square Institute of Neurology, University College London, London, UK

5 Wallenberg Centre for Molecular and Translational Medicine and the Department of Psychiatry and Neurochemistry, Institute of Neuroscience and Physiology, University of Gothenburg, 405 30 Gothenburg, Sweden

6 Dementia Research Centre, Queen Square Institute of Neurology, University College London, London, UK

7 UK Dementia Research Institute, Queen Square Institute of Neurology, University College London, London, UK

Correspondence to: Kerstin Sander

University College London, Centre for Radiopharmaceutical Chemistry, Kathleen Lonsdale Building, 5 Gower Place, London WC1E 6BS, UK

E-mail: k.sander@ucl.ac.uk

Abbreviations:

CBD – corticobasal degeneration

DLB – dementia with Lewy bodies

FTDP-17 – frontotemporal dementia with parkinsonism linked to chromosome 17

FTLD – frontotemporal lobar degeneration

MAO-B – monoamine oxidase B

MAPT – microtubule associated protein tau

NFT – neurofibrillary tangle

PHF – paired helical filament

PCA – posterior cortical atrophy

PSP – progressive supranuclear palsy

TDP-43 – TAR DNA-binding protein-43

Introduction

PET imaging of pathological inclusions of the microtubule associated protein tau (MAPT) in the human brain has the potential to enhance the accuracy of a dementia diagnosis in life, track disease progression and provide an outcome measure in clinical trials. Studies with the first tau targeting radiotracers, including the carbazole ^{18}F-flortaucipir (Tauvid^{TM}) and the arylquinolines of the THK series, provided evidence that tau PET can visualise pathological tau burden and propagation in patients with Alzheimer's disease.[1] However, the ability of these "first-generation" compounds to detect and discriminate tau inclusions in different primary tauopathies remains controversial. Furthermore, concerns have been raised about substantial off-target binding, in particular to the enzyme monoamine oxidase B (MAO-B), which may limit routine clinical applications.[2]

A new generation of tau PET tracers has recently been developed with the aim to overcome some of the limitations associated with the first-generation compounds, in particular to reduce MAO-B affinity and to improve the pharmacokinetic profile. Structurally, radiotracers like ^{18}F-PI2620 and ^{18}F-RO948 are carbazoles derived from ^{18}F-flortaucipir, whereas ^{18}F-MK6240 and ^{18}F-JNJ067 bear an isoquinolinamine core.[3–6] These new radiotracers have been optimised to have a high affinity for tau neurofibrillary tangles (NFTs) composed of paired helical filaments

3

(PHF) that are characteristic of Alzheimer's disease. Pilot PET studies suggest that the tracers are suitable for depicting pathological tau burden in Alzheimer's disease patients.[7–13] However, it remains unclear how structural differences between the tracers may affect sensitivity and specificity of binding to tau in its different forms in human brain.

Tracer validation studies in human *post-mortem* brain tissue are uniquely suited to bridge findings from clinical PET scans and neuropathological examinations as they allow assessment of tracer binding on a molecular level. The correct interpretation of clinical PET scans critically relies on the validation of the imaging agent. It is crucial to confirm that the radiotracer binds to a biological target that is representative of the underlying disease. With the aims of characterising, and comparing the binding profiles of structurally distinct, next-generation tau radiotracers, we carried out a head-to-head assessment of ^{3}H-PI2620, ^{3}H-RO948, ^{3}H-MK6240 and ^{3}H-JNJ067 in human *post-mortem* brain tissue from cases with a range of dementias and age-matched controls.

Materials and methods

Tissue selection

Ethical approval for the collection of *post-mortem* human brain tissue through the Queen Square Brain Bank for Neurological Disorders, University College London, was obtained from the National Research Ethics Service Committee London (Central: 08/H0718/54+5). Informed consent was obtained from each donor.

All cases underwent standard neuropathological assessment and were diagnosed according to standard criteria (Supplementary Table 1). Disease cases were included based on a high load of disease specific pathological protein burden in the frontal cortex. Demographic data is summarised in Table 1. The specificity of radiotracer binding was assessed in the frontal cortex

4

(Brodmann area 9) and medial temporal lobe (hippocampus, parahippacampal gyrus). Basal ganglia sections (including putamen, globus pallidus, caudate nucleus) from Alzheimer's disease cases were examined to detect potential off-target binding.

Immunohistochemistry on fresh frozen tissue sections

Staining with the phospho-tau specific antibody AT8 was carried out in sequential frozen tissue sections adjacent to those used for quantitative phosphorimaging as described previously.[14] In brief, tissue sections were incubated with AT8 (Thermoscientific, 1:600) for one hour at room temperature, followed by biotinylated anti-mouse IgG (DAKO, 1:200; 30 min) and avidin-biotin complex (VectorLaboratories; 30 min). Colour was developed with 3,3'-diaminobenzidine and hydrogen peroxide. Counterstaining was carried out using Mayer's haematoxylin. Immunostained slides were scanned on an Olympus VS120 slide scanner and pathological tau load was analysed using Olympus VS120 software.

Quantitative phosphorimaging

Quantitative phosphorimaging was carried out as described previously.[15] In brief, total tracer binding (TB) was determined using 5 nM ^{3}H-PI2620 (0.91 GBq/µmol), 3 nM ^{3}H-RO948 (0.94 GBq/µmol), 1 nM ^{3}H-MK6240 (1.69 GBq/µmol) and 10 nM ^{3}H-JNJ067 (2.71 GBq/µmol), respectively. Homologous blocking studies to determine the non-specific binding (NSB) were carried out using the non-radioactive analogues (10 µM PI2620, 10 µM RO948, 100 nM MK6240, 10 µM JNJ067). Heterologous blocking with L-deprenyl (1 µM) was carried out in basal ganglia sections. Following incubation, unbound tracer was removed using either saline or, in case of ^{3}H-JNJ067 (Supplementary Fig. 1), ethanol/phosphate-buffered saline. A detailed

5

protocol can be found in the Supplementary Material (Supplementary Table 2, Supplementary Protocol 1).

Data availability

Data that support the findings of this study are available from the corresponding author upon reasonable request.

Results

Pathological accumulation of hyperphosphorylated tau was confirmed by immunostaining with the phospho-tau specific antibody AT8 in frontal cortex sections directly adjacent to those used for quantitative phosphorimaging. In Alzheimer's disease cases, a high load of NFTs, neuropil threads and dystrophic neurites was detected in the grey matter. NFTs and threads were observed in the case with frontotemporal dementia with parkinsonism linked to chromosome 17 (FTDP-17) due to a *MAPT* R406W mutation. Pick's bodies and neuropil threads were found in Pick's disease cases. Cases with progressive supranuclear palsy (PSP) and corticobasal degeneration (CBD) exhibited neuronal inclusions in the grey matter as well as disease specific astroglial pathology (tufted astrocytes and coiled bodies in oligodendrocytes in PSP, astrocytic plaques in CBD). In two out of seven cases with sporadic primary tauopathies (PiD#12, PSP#14), concomitant Alzheimer's disease pathology was observed. Tau aggregates were not observed in the assessed sections of cases with non-tau proteinopathies, including dementia with Lewy bodies (DLB) and frontotemporal lobar degeneration linked to TAR DNA-binding protein-43 (FTLD-TDP), or in controls.

6

All four tau tracers were found to discriminate Alzheimer's disease cases as well as the FTDP-17 case with the *MAPT* R406W mutation from controls (Fig. 1). In contrast, there was no evidence of enhanced tau tracer binding to the frontal cortex of primary tauopathies with inclusions predominantly composed of either three-repeat tau (Pick's disease) or four-repeat tau isoforms (PSP, CBD), and non-tau proteinopathies (DLB, FTLD-TDP). In this group of diseases, total binding was low, and comparable to that found in control cases (Supplementary Fig. 2, Supplementary Table 3). An exception was the case PSP#14, where moderate tracer binding was observed with ^{3}H-MK6240 and ^{3}H-JNJ067 (*vide infra*).

In Alzheimer's disease, a high consistency between AT8 immunohistochemical staining and tau tracer binding was observed (Fig. 1A). Tracer binding occurred predominantly in the grey matter, with high global grey-to-white matter ratios. The specific binding to the grey matter of the Alzheimer's disease cases, including those clinically diagnosed with posterior cortical atrophy (PCA), was high for all four tau tracers (^{3}H-PI2620: 90±6%; ^{3}H-RO948: 97±1%; ^{3}H-MK6240: 88±4%; ^{3}H-JNJ067: 94±1%) (Fig. 1B). The average specific ^{3}H-PI2620 binding (1000±400 Bq/cm^2) was five times higher than in control cases (183 Bq/cm^2). Specific ^{3}H-RO948 binding in directly adjacent sections was found to be 690±250 Bq/cm^2, 15 times higher than the average specific binding determined in control cases (47 Bq/cm^2). Specific ^{3}H-MK6240 binding was determined to be 390±160 Bq/cm^2, which was 98 times higher than in control cases (4 Bq/cm^2). Finally, a high specific signal was measured for ^{3}H-JNJ067 binding to Alzheimer's disease cases (2300±1100 Bq/cm^2), compared to very low tracer binding – close to the lower limit of quantification – in control cases (<6 Bq/cm^2).

With the aim of confirming the specificity of the tau ligands for cortical tau inclusions composed of PHF, we assessed tracer binding to the frontal cortex of a FTDP-17 case with a *MAPT* R406W mutation (Fig. 1). This mutation gives rise to tau inclusions that morphologically resemble the type of pathology found in Alzheimer's disease, albeit at lower

7

density. Consistent with AT8 immunostaining, all four tau tracers showed elevated specific binding to the grey matter of this case (^{3}H-PI2620: 503 Bq/cm^2; ^{3}H-RO948: 247 Bq/cm^2; ^{3}H-MK6240: 263 Bq/cm^2; ^{3}H-JNJ067: 672 Bq/cm^2).

Intrigued by the positive signal observed in the frontal cortex of case PSP#14, but not in the remaining PSP and CBD cases, we hypothesised that the increased tracer binding is a result of the concomitant AD pathology found in PSP#14 (Table 1). To test this, we assessed tracer binding in medial temporal lobe sections of selected primary tauopathy cases, in comparison to control as well as Alzheimer's disease cases (Fig. 2; Supplementary Table 4). All cases, except the controls, were found to have a substantial amount of tau burden as indicated by AT8 immunostaining (Supplementary Fig. 3). Increased tracer binding, similar to that found in Alzheimer's disease cases (e.g. AD#4, PCA#9), was observed in the entorhinal cortex of case PiD#12 (Braak stage IV) as well as in the hippocampus and parahippocampal cortex of case PSP#14 (Braak stage V). In contrast, cases characterised as Braak stage 0, and with AT8 positive staining (PiD#11, PiD#13, PSP#15, CBD#16) were lacking specific tracer binding.

With the aim of assessing the specificity of tau tracer binding in the basal ganglia, we performed homogenous and heterogenous blocking studies using the non-radioactive analogue of each tracer and L-deprenyl, a selective MAO-B inhibitor, respectively (Fig. 3). In agreement with AT8 immunostaining, all four tau tracers were found to bind to the putamen, the globus pallidus and caudate nucleus. The signal was specific as demonstrated in self-block experiments, yet substantially lower than that detected in the adjacent insular cortex. In contrast, blocking of MAO-B binding sites with L-deprenyl did not result in tau tracer displacement.

Discussion

8

In this study, we used directly adjacent tissue sections from cases with a broad range of dementias allowing for a definite head-to-head comparison of four next-generation tau PET tracers as well as validation of the target specificity of each tracer investigated. In line with recently reported studies, the cortical binding profiles of the four tracers were comparable in that the compounds were found to distinguish Alzheimer's disease cases from controls,[7–13] primary tauopathies characterised by tau inclusions predominantly composed of three- or four-repeat tau isoforms and dementias with underlying TDP-43 and α-synuclein pathology with high robustness.[16,17] The strong signal obtained in Alzheimer's disease cases as well as in the *MAPT* R406W mutation case confirms that the new tracers depict PHF-tau with high specificity. The binding profile of the new tau tracers is highly comparable to that observed with ^{18}F-flortaucipir and its fluorescent analogue T726, which has been found to bind to neuropil threads, pre-tangles and a subset of neurofibrillary tangles.[14,15] As observed previously with ^{18}F-flortaucipir[15] as well as ^{18}F-THK5117,[14] there was a high variability in next generation tau tracer binding in the Alzheimer's disease cases; yet, the relative spread was similar for all four tracers investigated, and is most likely a reflection of individual differences in tau burden. Our results support the notion that all four tracers are suited to diagnose Alzheimer's disease in life. Ultimately, this may be beneficial for future multicentre studies as data from patient cohorts scanned with different tau tracers may be pooled.

High grey-to-white matter ratios in the Alzheimer's disease cases reflect radiotracer binding to the cortical neurons that are most affected, and are in good agreement with the excellent contrast observed in human PET scans.[1] The tracers were found to differ in the ratio between specific binding in Alzheimer's disease compared to control cases (^{3}H-MK6240>^{3}H-RO948>^{3}H-PI2620). A large margin between disease and healthy tissue can potentially permit detection of small changes in pathological tau load, which is of particular interest when assessing novel therapeutic interventions. The binding profile of the isoquinolinamine ^{3}H-

9

JNJ067 was found to be similar to that of ^{3}H-MK6240; however, it must be noted that the higher lipophilicity of JNJ067 (LogP=3.18, compared to 2.24 for MK6240, and 2.57 for the carbazoles) prevented the use of the physiological assay conditions. This precludes direct comparison of the binding profile of JNJ067 with the other tracers as the experimental conditions used will have exaggerated the apparent specific binding of this tracer. Whilst higher lipophilicity is associated with increased non-specific binding,[18] it should be noted that the four tracers were used at different concentrations (up to five-fold variation) and with different washing conditions (*cf.* Supplementary Material), to allow testing with similar levels of radioactivity. The specific and non-specific binding of each tracer will therefore to some extent reflect their respective molar activity, precluding direct comparison of the different data sets, yet such effects are unlikely to have affected the overall trends reported.

We observed enhanced tracer binding in the frontal cortex of one of two PSP cases studied (PSP#14) and in the medial temporal lobe of cases PiD#12 and PSP#14. Given the concomitant Alzheimer's disease pathology in these cases, combined with low tracer binding in other primary tauopathy cases (incommensurate with substantial tau load as indicated by AT8 immunostaining), it is likely that this binding reflects the high sensitivity and specificity of these tracers to depict PHF-tau. Cortical ^{18}F-PI2620 binding in PSP has been observed,[3,19] albeit in a subset of cases and patients and at a lower signal intensity than in Alzheimer's disease cases and patients. Given the spread of tau load in the sporadic primary tauopathies, in particular PSP, a larger sample size would be needed to rule out any binding to this disease group. However, the lack of robust cortical tracer binding suggests that the tracers investigated do not have sufficiently high affinity for the cortical tau inclusions characteristic of these diseases and therefore, caution is required for the interpretation of clinical scans.

Off-target binding is a major limitation associated with the first-generation tau radioligands. In particular, the basal ganglia were found to be affected by extensive binding to MAO-B.[20] We

10

observed low binding of the new tau radiotracers to selected regions of interest, including putamen, globus pallidus and caudate nucleus, in Alzheimer's disease cases. Tracer uptake patterns and signal strength were in good visual alignment with AT8 immunostaining. Tracer binding was not displaceable by the MAO-B inhibitor L-deprenyl, confirming a trend observed by others *in vitro* and *in vivo*,[6,9,16,21] and providing evidence that MAO-B is not a significant binding target for the new tau radiotracers. This is particularly important for future studies assessing the specificity of basal ganglia binding in the primary tauopathies.[19]

In conclusion, this head-to-head comparison of the next-generation tau radiotracers ^{3}H-PI2620, ^{3}H-RO948, ^{3}H-MK6240 and ^{3}H-JNJ067 in human *post-mortem* brain tissue demonstrates that all four radiotracers bind with high specificity to cortical PHF-tau, whereas tracer binding to cortical inclusions characteristic of primary tauopathies is low. Several limitations of the first generation of tau tracers, largely associated with MAO-B off-target binding, appear to have been overcome. Our results suggest that the new tau PET tracers are suitable tools for distinguishing Alzheimer's disease from controls as well as other dementias (with the exception of MAPT mutations causing PHF-tau pathology) with high robustness.

11

Centre (MCW), an Alzheimer's Research UK Senior Fellowship (TL) and Mallinckrodt Pharmaceuticals (KS). The work was undertaken at the UCL Centre for Radiopharmaceutical Chemistry, and the Dementia Research Centre which are funded in part by the Department of Health's NIHR Biomedical Research Centres funding scheme. The Queen Square Brain Bank is supported by the Reta Lila Weston Institute for Neurological Studies.

Competing interests

The authors declare no competing interests.

Supplementary material

Supplementary data will be made available with the online version.

12

References

1. Schöll M, Maass A, Mattsson N, *et al*. Biomarkers for tau pathology. *Mol Cell Neurosci*. 2019;97:18-33.

2. Leuzy A, Chiotis K, Lemoine L, *et al*. Tau PET imaging in neurodegenerative tauopathies - still a challenge. *Mol Psychiatry*. 2019;24(8):1112-1134.

3. Kroth H, Oden F, Molette J, *et al*. Discovery and preclinical characterization of [^{18}F]PI-2620, a next-generation tau PET tracer for the assessment of tau pathology in Alzheimer's disease and other tauopathies. *Eur J Nucl Med Mol Imaging*. 2019;46(10):2178-2189.

4. Honer M, Gobbi L, Knust H, *et al*. Preclinical Evaluation of ^{18}F-RO6958948, ^{11}C-RO6931643, and ^{11}C-RO6924963 as novel PET radiotracers for imaging tau aggregates in Alzheimer disease. *J Nucl Med*. 2018;59(4):675-681.

5. Hostetler ED, Walji AM, Zeng Z, *et al*. Preclinical characterization of ^{18}F-MK-6240, a promising PET tracer for in vivo quantification of human neurofibrillary tangles. *J Nucl Med*. 2016;57(10):1599-1606.

6. Rombouts FJR, Declercq L, Andrés JI, *et al*. Discovery of *N*-(4-[^{18}F]fluoro-5-methylpyridin-2-yl)isoquinolin-6-amine (JNJ-64326067), a new promising tau positron emission tomography imaging tracer. *J Med Chem*. 2019;62(6):2974-2987.

7. Kuwabara H, Comley RA, Borroni E, *et al*. Evaluation of ^{18}F-RO-948 PET for quantitative assessment of tau accumulation in the human brain. *J Nucl Med*. 2018;59(12):1877-1884.

8. Pascoal TA, Shin M, Kang MS, *et al*. In vivo quantification of neurofibrillary tangles with [^{18}F]MK-6240. *Alzheimers Res Ther*. 2018;10(1):74.

9. Betthauser TJ, Cody KA, Zammit MD, *et al*. In vivo characterization and quantification of neurofibrillary tau PET radioligand ^{18}F-MK-6240 in humans from Alzheimer disease dementia to young controls. *J Nucl Med*. 2019;60(1):93-99.

10. Lohith TG, Bennacef I, Vandenberghe R, *et al*. Brain imaging of Alzheimer dementia patients and elderly controls with ^{18}F-MK-6240, a PET tracer targeting neurofibrillary tangles. *J Nucl Med*. 2019;60(1):107-114.

11. Mormino EC, Toueg TN, Azevedo C, *et al*. Tau PET imaging with ^{18}F-PI-2620 in aging and neurodegenerative diseases [published online June 23, 2020]. *Eur J Nucl Med Mol Imaging*. doi:10.1007/s00259-020-04923-7

12. Mueller A, Bullich S, Barret O, *et al*. Tau PET imaging with ^{18}F-PI-2620 in patients with Alzheimer disease and healthy controls: a first-in-humans study. *J Nucl Med*. 2020;61(6):911-919.

13. Schmidt ME, Janssens L, Moechars D, *et al*. Clinical evaluation of [^{18}F]JNJ-64326067, a novel candidate PET tracer for the detection of tau pathology in Alzheimer's disease. *Eur J Nucl Med Mol Imaging*. 2020;47(13):3176-3185.

14. Wren MC, Lashley T, Årstad E, Sander K. Large inter- and intra-case variability of first generation tau PET ligand binding in neurodegenerative dementias. *Acta Neuropathol Commun*. 2018;6(1):34.

15. Sander K, Lashley T, Gami P, *et al*. Characterization of tau positron emission tomography tracer [^{18}F]AV-1451 binding to postmortem tissue in Alzheimer's disease, primary tauopathies, and other dementias. *Alzheimers Dement*. 2016;12(11):1116-1124.

16. Aguero C, Dhaynaut M, Normandin MD, *et al*. Autoradiography validation of novel tau PET tracer [F-18]-MK-6240 on human postmortem brain tissue. *Acta Neuropathol Commun*. 2019;7(1):37.

14

17. Leuzy A, Smith R, Ossenkoppele R, *et al*. Diagnostic performance of RO948 F 18 tau positron emission tomography in the differentiation of Alzheimer disease from other neurodegenerative disorders. *JAMA Neurol*. 2020;77(8):955-965.

18. Oi N, Tokunaga M, Suzuki M, *et al*. Development of novel PET probes for central 2-amino-3-(3-hydroxy-5-methyl-4-isoxazolyl)propionic acid receptors. *J Med Chem*. 2015;58(21):8444-8462.

19. Brendel M, Barthel H, van Eimeren T, *et al*. Assessment of ^{18}F-PI-2620 as a biomarker in progressive supranuclear palsy. *JAMA Neurol*. 2020;77(11):1408-1419.

20. Saint-Aubert L, Lemoine L, Chiotis K, Leuzy A, Rodriguez-Vieitez E, Nordberg A. Tau PET imaging: present and future directions. *Mol Neurodegener*. 2017;12(1):19.

21. Smith R, Schöll M, Leuzy A, *et al*. Head-to-head comparison of tau positron emission tomography tracers [^{18}F]flortaucipir and [^{18}F]RO948. *Eur J Nucl Med Mol Imaging*. 2020;47(2):342-354.

15

Figure Legends

Figure 1. Binding of the tau tracers ^{3}H-PI2620, ^{3}H-MK6240, ^{3}H-RO948 and ^{3}H-JNJ067 to the frontal cortex from age-matched controls, Alzheimer's disease cases, a FTDP-17 case with a *MAPT* R406W mutation and PSP cases. **A)** Immunohistochemistry with AT8 and tracer binding in adjacent tissue sections of representative cases. Scale bar = 10 mm. **B**) Total (closed circles) and non-specific (open circles) tracer binding to the grey matter expressed in Bq/cm^2.

Abbreviations: CTRL, age-matched control; AD, Alzheimer's disease; R406W, frontotemporal dementia with parkinsonism linked to chromosome 17 due to a missense mutation in the microtubule-associated protein tau gene (MAPT); PSP, progressive supranuclear palsy; GM/WM, grey-to-white matter ratio based on total tracer binding in these areas of interest.

Figure 2. Binding of the tau tracers ^{3}H-PI2620, ^{3}H-MK6240, ^{3}H-RO948 and ^{3}H-JNJ067 to the medial temporal lobe from selected cases with primary tauopathies, Alzheimer's disease cases and age-matched controls. Immunohistochemistry with AT8 and tracer binding in adjacent tissue sections of representative cases. Scale bar = 5 mm.

Abbreviations: CTRL, age-matched control; AD, Alzheimer's disease; PiD, Pick's disease, PSP, progressive supranuclear palsy; CBD, corticobasal degeneration.

Figure 3. Comparison of carbazole (^{3}H-PI2620, ^{3}H-RO948) and isoquinolinamine (^{3}H-MK6240, ^{3}H-JNJ067) bearing tau tracers to basal ganglia sections from Alzheimer's disease cases. Representative images showing immunohistochemistry staining with AT8 (**A**), total tracer binding (**B**), self-block with the non-radiolabelled analogue of each tracer (**C**) and MAO-B inhibition with L-deprenyl (**D**). Scale bar = 10 mm.

16

Abbreviations: AD, Alzheimer's disease; TB, total binding; NSB, non-specific binding after self-block; DEP, L-deprenyl block.

17

Table 1 Demographic data

Neuropathological diagnosis	Case ID	AAO	AAD	BW, g	Gender	Braak	Thal	ABC
CTRL	1	N/A	86	1230	F	I	4	A3B1C1
CTRL	2	N/A	95	1346	M	I	1	A1B1C1
AD	3	57	76	1303	F	VI	5	A3B3C2
AD	4	63	79	1423	M	VI	5	A3B3C3
AD	5	48	63	1042	M	VI	5	A3B3C3
AD	6	63	73	1269	M	VI	5	A3B3C3
AD	7	63	74	1022	M	VI	5	A3B3C3
AD (PCA)	8	55	68	1126	F	VI	5	A3B3C3
AD (PCA)	9	57	65	1121	F	VI	5	A3B3C3
R406W	10	55	66	1208	M	0	0	A0B0C0
PiD	11	52	62	1123	M	0	0-1	A1B0C0
PiD	12	60	67	1470	M	IV	4	A3B3C2
PiD	13	52	67	982	M	0	2	A1B0C0
PSP	14	57	62	1369	M	V	5	A3B3C2
PSP	15	76	84	1370	M	0	4	A3B0C1
CBD	16	57	64	1456	M	0	0	A0B0C0
CBD	17	54	61	1389	M	0	0	A0B0C0
DLB	18	59	75	1123	M	II	1	A1B1C1
DLB	19	79	89	1258	F	III	5	A3B2C2
TDPA	20	66	72	1274	M	0	1	A1B0C0
TDPA	21	51	61	1065	M	I	3	A1B1C0
TDPC	22	73	83	1167	M	II	2	A1B1C1
TDPC	23	54	71	1363	M	0	0	A0B0C0
C9Orf72	24	64	73	1252	M	IV	3	A2B2C1
C9Orf72	25	52	58	1303	M	I	3	A2B1C1

AAD = age at death; AAO = age at onset; AD = Alzheimer's disease; BW = brain weight; *C9orf72* = frontotemporal lobar degeneration due to a mutation in *C9orf72*; CBD = corticobasal degeneration; CTRL = age-matched control; DLB = dementia with Lewy bodies; M/F = male/female.; N/A = not applicable; PCA = posterior cortical atrophy; PiD = Pick's disease; PSP = progressive supranuclear palsy; R406W = frontotemporal dementia with parkinsonism linked to chromosome 17 due to a missense mutation on the microtubule-associated protein tau; TDPA/C = frontotemporal lobar degeneration linked to TDP-43 type A/C.
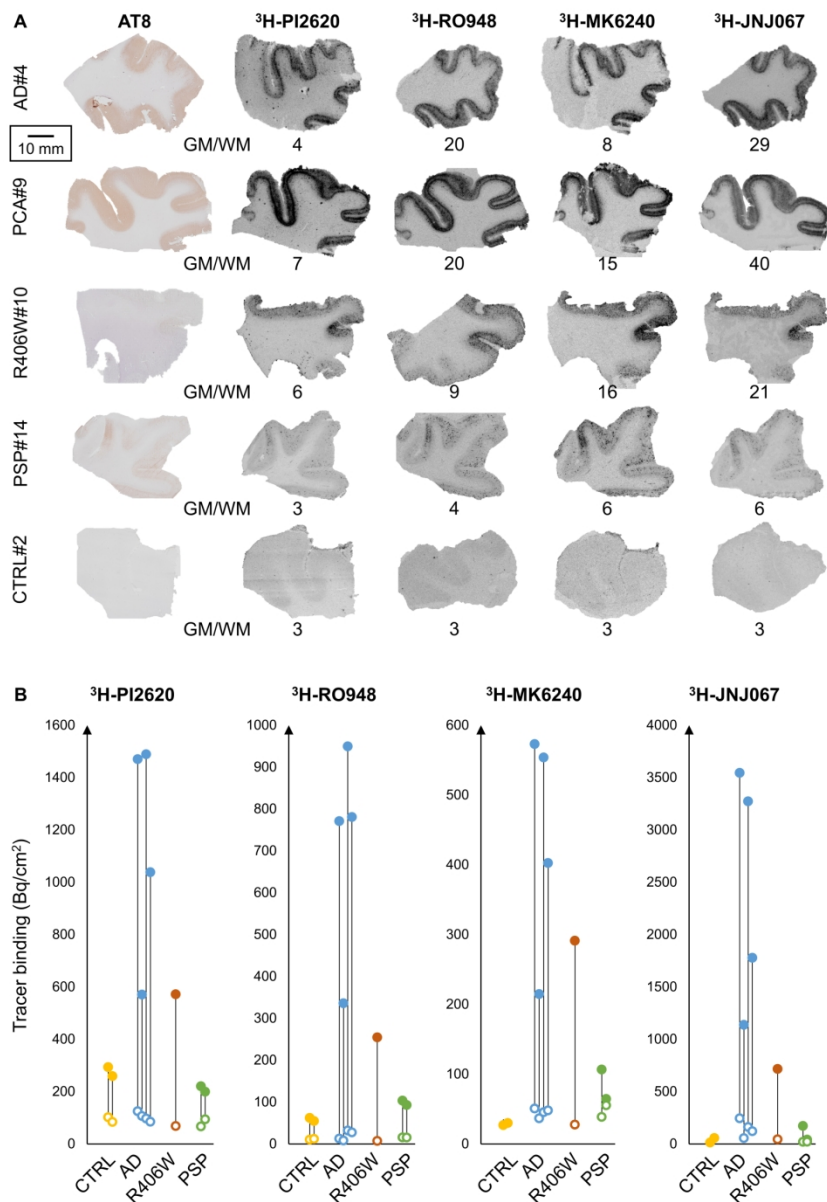
Figure 1. Binding of the tau tracers ^{3}H-PI2620, ^{3}H-MK6240, ^{3}H-RO948 and ^{3}H-JNJ067 to the frontal cortex from age-matched controls, Alzheimer's disease cases, a FTDP-17 case with a *MAPT* R406W mutation and PSP cases. **A**) Immunohistochemistry with AT8 and tracer binding in adjacent tissue sections of representative cases. Scale bar = 10 mm. **B**) Total (closed circles) and non-specific (open circles) tracer binding to the grey matter expressed in Bq/cm^{2}.

Abbreviations: CTRL, age-matched control; AD, Alzheimer's disease; R406W, frontotemporal dementia with parkinsonism linked to chromosome 17 due to a missense mutation in the microtubule-associated protein tau gene (*MAPT*); PSP, progressive supranuclear palsy; GM/WM, grey-to-white matter ratio based on total tracer binding in these areas of interest.
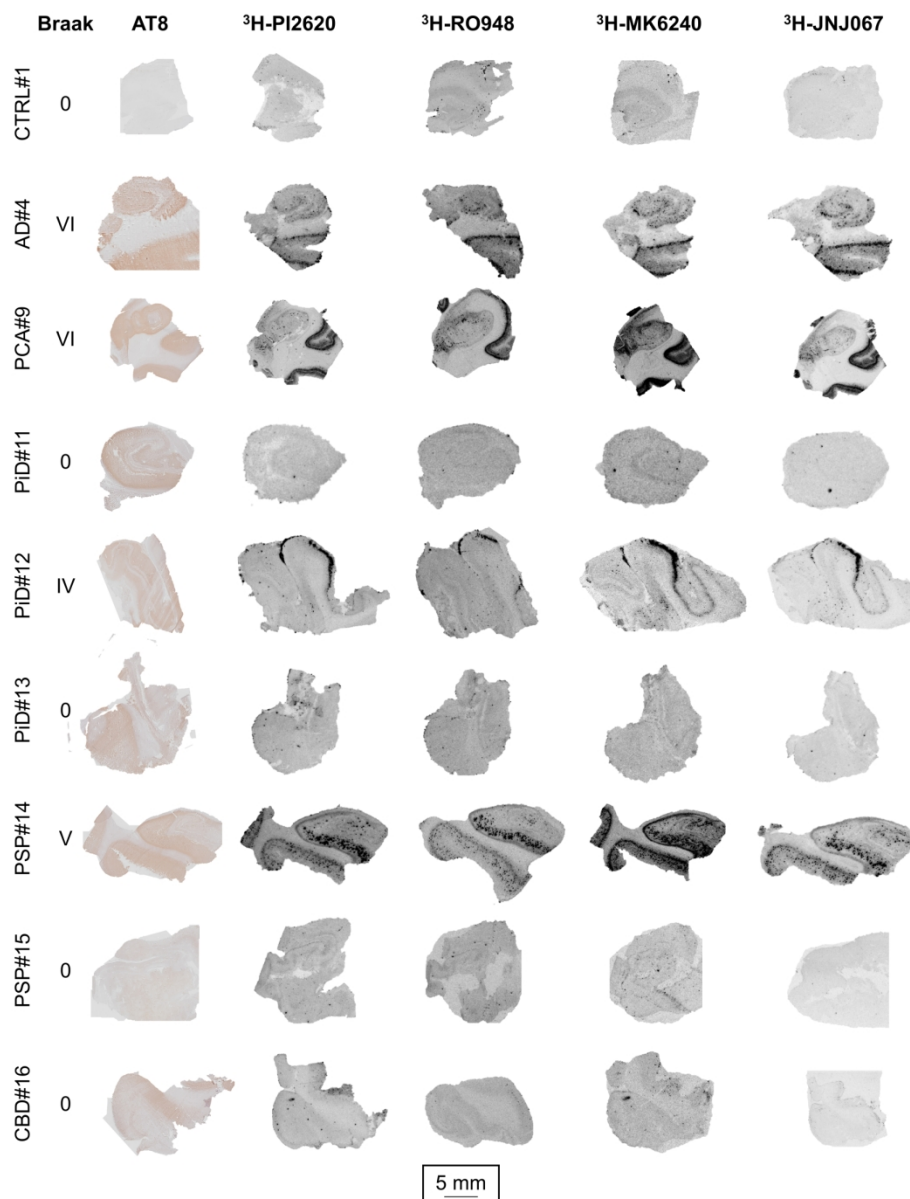
38x55mm (1109 x 1109 DPI)

Figure 2. Binding of the tau tracers ^{3}H-PI2620, ^{3}H-MK6240, ^{3}H-RO948 and ^{3}H-JNJ067 to the medial temporal lobe from selected cases with primary tauopathies, Alzheimer's disease cases and age-matched controls. Immunohistochemistry with AT8 and tracer binding in adjacent tissue sections of representative cases. Scale bar = 5 mm.
Abbreviations: CTRL, age-matched control; AD, Alzheimer's disease; PiD, Pick's disease, PSP, progressive supranuclear palsy; CBD, corticobasal degeneration.
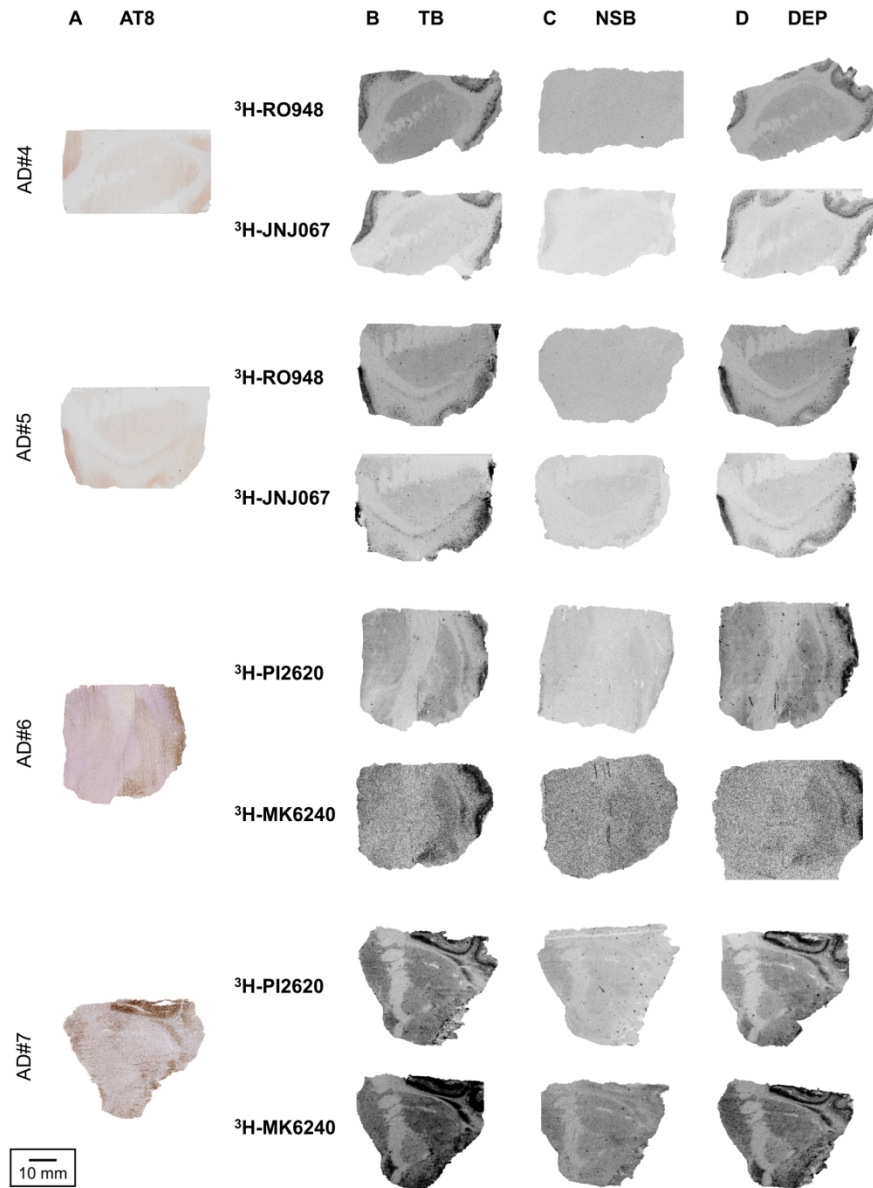
38x49mm (1164 x 1164 DPI)

Figure 3. Comparison of carbazole (^{3}H-PI2620, ^{3}H-RO948) and isoquinolinamine (^{3}H-MK6240, ^{3}H-JNJ067) bearing tau tracers to basal ganglia sections from Alzheimer's disease cases. Representative images showing immunohistochemistry staining with AT8 (**A**), total tracer binding (**B**), self-block with the non-radiolabelled analogue of each tracer (**C**) and MAO-B inhibition with L-deprenyl (**D**). Scale bar = 10 mm. *Abbreviations:* AD, Alzheimer's disease; TB, total binding; NSB, non-specific binding after self-block; DEP, L-deprenyl block.

38x52mm (1141 x 1141 DPI)

To determine the binding profiles of next-generation tau PET tracers, Yap *et al.* performed a head-to-head comparison of four new compounds in human post-mortem brain tissue. The results suggest that the four tracers are equally well-suited to discriminating Alzheimer's disease from other dementias and from controls.